ELSEVIER

International Journal of Mass Spectrometry 225 (2003) 25–37

International Journal of Mass Spectrometry

www.elsevier.com/locate/ijms

Electron-impact ionization of NO, NO_2, and N_2O

J. Lopez, V. Tarnovsky, M. Gutkin, K. Becker*

Department of Physics and Engineering Physics, Stevens Institute of Technology, Hoboken, NJ 07030, USA

Received 28 August 2002; accepted 7 October 2002

Abstract

We measured absolute cross-sections for the electron-impact ionization and dissociative ionization of the three nitrogen–oxygen compounds NO, NO_2, and N_2O from threshold to 200 eV using the fast-neutral-beam technique. In spite of the importance of these molecules in combustion, low-temperature plasmas, pollution control, and planetary atmospheres, the database of absolute total and partial electron-impact ionization cross-sections for these species is not very comprehensive and existing data reveal some discrepancies. To the best of our knowledge, this is the first time that absolute partial ionization cross-sections for all three species have been measured by the same group using the same experimental technique and apparatus. Comparisons with other available measured and calculated ionization cross-section data are made.

Keywords: Electron-impact ionization; Cross-sections; NO_x; Pollution control; Combustion; Atmospheric chemistry

1. Introduction

The oxides of nitrogen, nitric oxide (NO) and nitrogen dioxide (NO_2), along with nitrous oxide (N_2O), are among the most important molecules in atmospheric chemistry. In the stratosphere, NO_x reaction cycles are important mechanisms in the formation and maintenance of ozone. Ozone (O_3) in the stratosphere is an essential shield that protects living organisms from biologically harmful ultraviolet radiation. The principal natural source of NO and NO_2 in the stratosphere is N_2O [1]. Although these molecules are essential contributors to the chemistry in the upper atmosphere, they are undesirable pollutants in the troposphere. NO and NO_2 in the troposphere are increasingly formed due to the high temperatures of combustion of fuels with air that dissociate oxygen (O_2) and nitrogen (N_2) molecules into their atomic constituents, which subsequently recombine [2]. In ambient air, the oxides of nitrogen together with hydrocarbons are among the major causes of photochemically produced smog [3]. N_2O, which is emitted predominately by biological sources in soil and water, is an extremely powerful greenhouse gas which acts as an atmospheric thermal insulator [4].

Due to the atmospheric and environmental importance of the molecules NO, NO_2, and N_2O many previous studies have been carried out to elucidate their atomic and molecular properties and their interactions with photons and electrons. However, only a few previous measurements of the ionization properties of these molecules have been reported in the literature to date. Previous work on the ionization properties of these molecules include the early work of Rapp and Englander-Golden [5], Märk and co-workers [6–8],

* Corresponding author.
E-mail address: kbecker@stevens-techn.edu (K. Becker).

1387-3806/02/$ – see front matter
PII S1387-3806(02)01042-4

Iga et al. [9], and the more recent studies of Lindsay et al. [10], Lukic et al. [11], and Jiao et al. [12]. Calculated total single ionization cross-sections for all three targets have also been reported using the BEB formalism of Kim and co-workers [13,14] and in the case of NO_2 another calculated cross-section based on the Deutsch–Märk (DM) formalism has been reported [15].

In this paper, we report absolute partial cross-sections for the electron-impact ionization and dissociative ionization of the three nitrogen–oxygen compounds NO, NO_2, and N_2O from threshold to 200 eV using the fast-neutral-beam technique. To the best of our knowledge, this is the first time that ionization cross-sections for all three targets have been measured in the same apparatus using the same experimental technique. Detailed comparisons are made with other available experimental data and with the published calculated total single ionization cross-sections.

2. Experimental technique

A detailed description of the fast-beam apparatus and of the experimental procedure employed in the determination of absolute partial ionization cross-sections has been given in previous publications from this laboratory [16–20]. The primary ion source is a commercially available Colutron ion source which is operated in the standard mode where a dc discharge is ignited between a heated filament and an anode through the properly chosen feed gas. In the present experiments, NO, NO_2, and N_2O gases were obtained from Matheson Gas Products in the highest commercially available purity and used without further purification. For each target gas, positively charged primary ions were extracted from the ion source, accelerated to about 3 keV, mass selected in a Wien filter, and sent through a charge-transfer cell filled with a suitably chosen charge-transfer gas for resonant or near-resonant charge transfer of a fraction of the primary ions. Xe with ionization energy of 12.14 eV [21,22] was found to be an appropriate charge neutralization target. The residual ions in the beam were removed from the neutral target gas beam by electrostatic deflection and most species in Rydberg states were quenched in a region of high electric field.

The fast neutral targets beam were subsequently crossed at right angles by a well-characterized electron beam (5–200 eV beam energy, 0.5 eV FWHM energy spread, 0.03–0.4 mA beam current). The product ions were focused in the entrance plane of an electrostatic hemispherical analyzer which separates ions of different charge-to-mass ratios (i.e., parent ions from fragment ions). The ions leaving the analyzer were detected by a channel electron multiplier (CEM). Absolute calibration of the relative cross-sections can be achieved in two ways. The fast-beam apparatus affords the capability to measure all quantities that determine the absolute cross-section directly. The target density, which is perhaps the most difficult quantity to determine, is obtained from the energy deposited by the fast target beam into a pyroelectric detector, which is first calibrated relative to a well-characterized ion beam [18,20]. As an alternative, the well-established Kr or Ar absolute ionization cross-sections can be used to calibrate the pyroelectric crystal. The calibrated detector, in turn, is then used to determine the flux of the neutral target beam in absolute terms. The second procedure avoids the frequent and prolonged exposure of the sensitive pyroelectric crystal to fairly intense ion beams [19,20].

We established that all fragment ions produced by dissociative ionization of the three compounds NO, NO_2, and N_2O with an excess kinetic energy of less than about 3.5 eV per fragment ion are collected and detected with 100% efficiency using a combination of in situ experimental studies and ion trajectory modeling calculations [16,23]. However, in the case of the N^+ and O^+ fragment ions we were not able to fully resolve the corresponding ion signals at the detector because of the well-known fact that these fragment ions are formed with broad distributions of excess kinetic energies with maximum excess kinetic energy values of up to 5 eV [10,11,13]. Furthermore, careful threshold studies revealed little evidence of the presence of excited target species (vibrationally excited

species, metastables, and species in high-lying Rydberg states) in the incident neutral beams in all three cases. The absolute cross-sections reported here were determined with uncertainties of ±15% for the parent ionization cross-section and ±18% for the dissociative ionization cross-section. These error margins, which are similar to what we quoted previously for ionization cross-sections measured for other free radicals in the same apparatus [16,17], include statistical uncertainties and all known sources of systematic uncertainties.

3. Results and discussion

In this section, we present our measured ionization cross-section data for the three target molecules along with detailed comparisons with other available experimental and calculated ionization cross-sections. In the case of the N^+ and O^+ fragment ions, we only report absolute cross-sections for the formation of $N^+ + O^+$ as we are unable to fully resolve the respective N^+ and O^+ ion signals at the detector because of the appreciable excess kinetic energy distributions with which these two atomic fragment ions are formed in all three cases (see discussion earlier).

3.1. Ionization cross-sections for NO

The diatomic molecule NO has one unpaired electron and may thus be classified chemically as a free radical [24]. It is, however, a rather stable molecule [25]. Fig. 1 shows the partial NO electron-impact ionization cross-sections measured as part of the present work. The electron-impact ionization of NO is clearly dominated by the formation of the parent NO^+ ions. As discussed above, we were not able to resolve the ion signals corresponding respectively to the N^+ and the O^+ fragment ions. Thus, we only give a partial cross-section for the combined formation of N^+ and O^+ ions. Also shown in Fig. 1 is the sum of the two measured partial cross-sections which represents the total single NO ionization cross-section

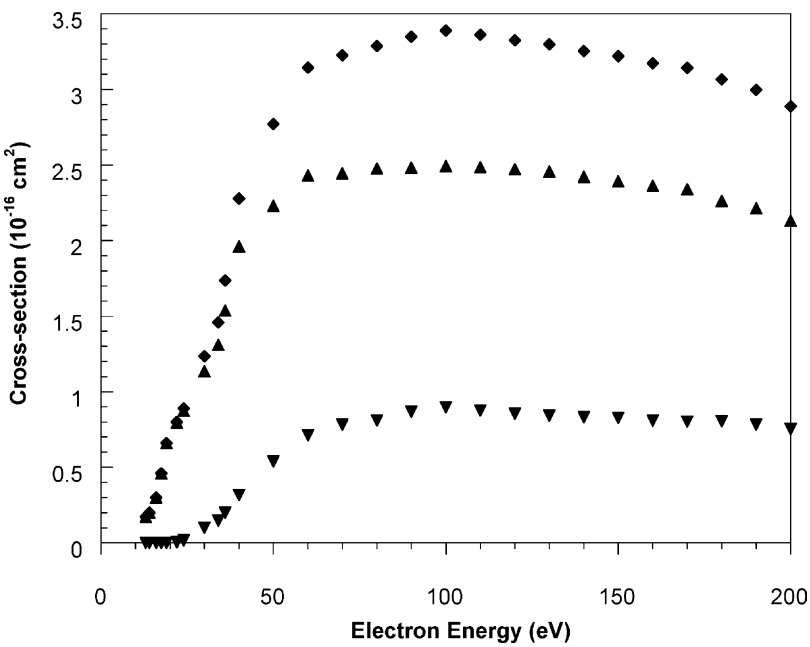

Fig. 1. Present NO^+ (▲) and combined ($N^+ + O^+$) (▼) partial electron-impact ionization cross-sections of NO as a function of electron energy from threshold to 200 eV. Also shown is the sum of the two cross-sections (◆), which represents the total single NO ionization cross-section, which is essentially identical to the total NO ionization cross-section (see text, for details).

(which is essentially identical to the total NO ionization cross-section as the cross-sections for the formation of multiply charged parent or fragment ions are much smaller than those for the formation of singly charged ions). Fig. 2 shows our measured partial NO^+ cross-section in comparison with data reported by Kim et al. [6], Iga et al. [9], and Lindsay et al. [10]. The peak cross-section values show a significant level of disagreement between the maximum value reported by Iga et al. [9], 3×10^{-16} cm^2, and the minimum value reported by Lindsay et al. [10], 2×10^{-16} cm^2. The present data and the data of Kim et al. [6] agree in terms of the maximum cross-section value (2.5×10^{-16} cm^2), but show a significant difference in the cross-section shape with the cross-section shape of Kim et al. [6] declining much more rapidly with increasing electron energy. Fig. 3 shows our combined ($N^+ + O^+$) partial ionization cross-section for the dissociative ionization of NO in comparison with the same cross-sections reported by Iga et al. [9] and Lindsay et al. [10]; we note that Kim et al. [6] only reported parent ionization cross-section data for NO, but no dissociative ionization cross-sections. The dissociative ionization cross-section measured here is similar in magnitude to that reported in [10], but shows somewhat different energy dependence. Both cross-sections are significantly larger than the one reported by Iga et al. [9], which maybe due to the fact that discrimination effects prevented these authors from collecting all energetic N^+ and O^+ fragment ions with 100% efficiency.

Fig. 4 shows our total single NO ionization cross-section in comparison with the measured data from [9,10] and with the total NO ionization cross-section reported by Rapp and Englander-Golden [5]. Also shown is the calculated NO cross-section from [13] using the BEB formalism. The maximum values of the reported measured cross-sections range from 2.7×10^{-16} cm^2 [10] to 3.6×10^{-16} cm^2 [9], a spread of about 30% which is slightly larger than the combined error margins of the cross-sections as reported in the original papers. The present cross-section data are very close both in terms of the cross-section maximum (3.4×10^{-16} cm^2) and in terms of the cross-section shape to the data reported by Iga et al. [9]. The calculated cross-section of Kim and co-workers

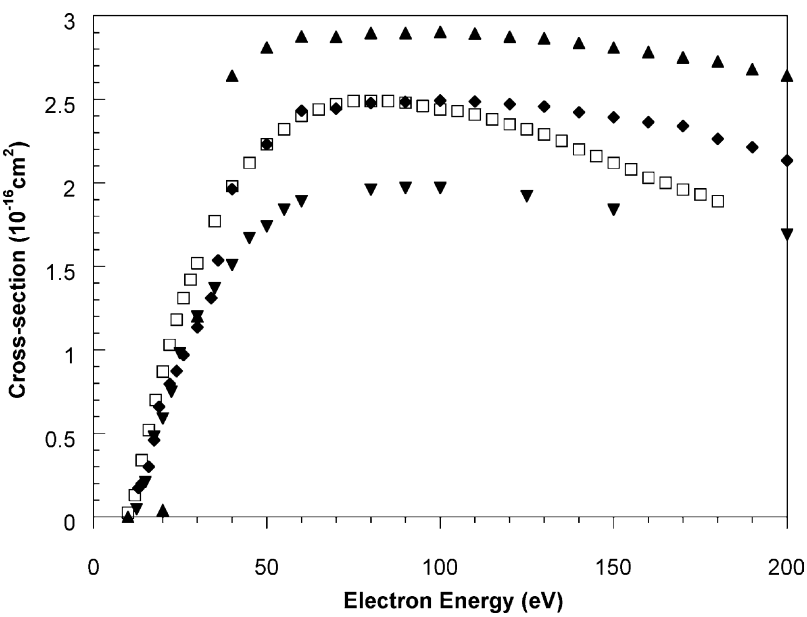

Fig. 2. Present NO^+ partial ionization cross-section of NO from threshold to 200 eV (◆) in comparison with the same cross-section from [6] (□), [9] (▲), and [10] (▼).

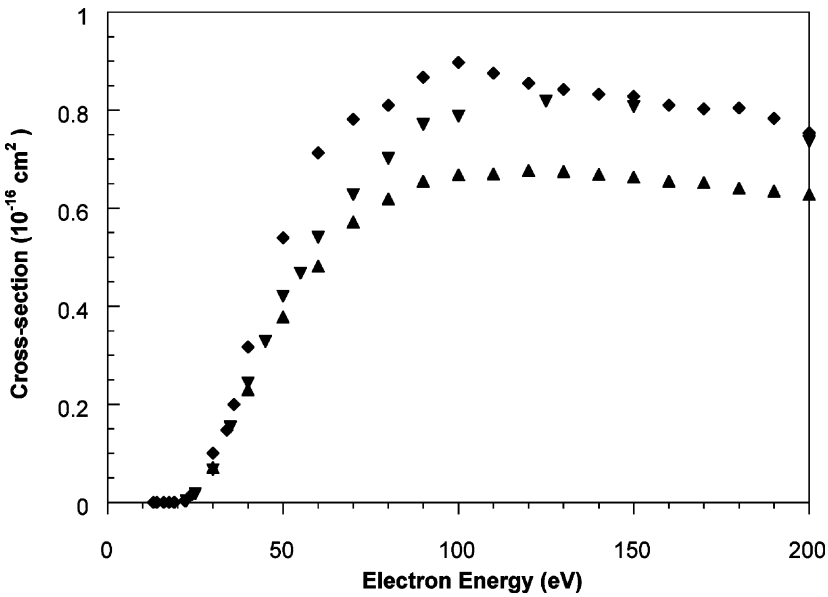

Fig. 3. Present ($N^+ + O^+$) partial ionization cross-section of NO from threshold to 200 eV (◆) in comparison with the same cross-section from [9] (▲) and [10] (▼).

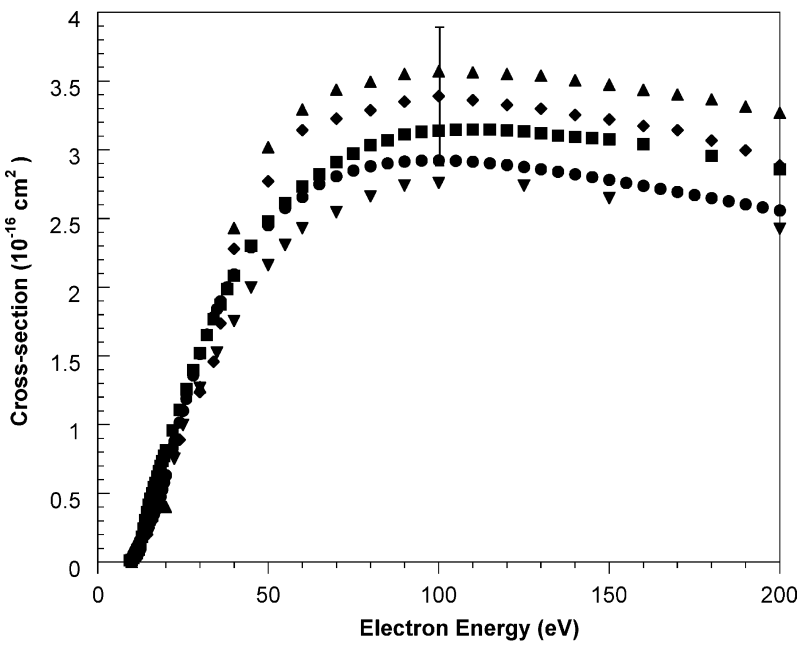

Fig. 4. Present total (single) NO ionization cross-section from threshold to 200 eV (◆) in comparison with the same measured cross-section from [9] (▲) and [10] (▼), the total measured NO ionization cross-section of Rapp and Englander-Golden [5] (■), and the calculated NO ionization cross-section of [13] (●). The single error bar refers to a typical margin of uncertainty in the present cross-section.

[13] shows a shape that is very similar to those of the two experimentally determined cross-sections, but its cross-section maximum is somewhat lower (2.9×10^{-16} cm^2). The recent data of Lindsay et al. [10] are below all other reported data and their cross-section shape is also different from all other reported cross-section shapes. The measured total NO cross-section of [5] has a maximum value of about 3.2×10^{-16} cm^2, but the cross-section declines much more gradually with increasing impact energy as the other cross-sections shown in Fig. 4. Overall, the level of agreement in the reported NO ionization cross-sections is not as good as one would expect for the case of a simple diatomic molecule where different measurements and calculations are often found to agree to better than 10% [26].

3.2. Ionization cross-sections for NO_2

NO_2 is a symmetrical, nonlinear triatomic molecule with a bond angle of 134° that has one unpaired electron, which classifies it chemically as a free radical [24]. Fig. 5 shows the partial NO_2 electron-impact ionization cross-sections measured as part of the present work. In contrast to NO, the ionization of NO_2 is dominated by dissociative ionization. The formation of NO^+ fragment ions has the largest partial ionization cross-section. The cross-section for the formation of the ($N^+ + O^+$) fragment ions, which as for NO could not be resolved, is larger than the parent $NO_2{}^+$ ionization cross-section for impact energies above about 50 eV; at lower impact energies the $NO_2{}^+$ parent ionization cross-section exceeds the ($N^+ + O^+$) partial cross-section because of the much lower threshold for the formation of the parent ions. Also shown in Fig. 5 is the sum of the measured $NO_2{}^+$ parent ionization cross-sections and the other partial ionization cross-section which represent the total single NO_2 ionization cross-section (which is essentially identical to the total NO_2 ionization cross as the cross-sections for the formation of multiply charged parent or fragment ions are much smaller than those for the formation of singly charged ions). Fig. 6 shows the present results for the formation of

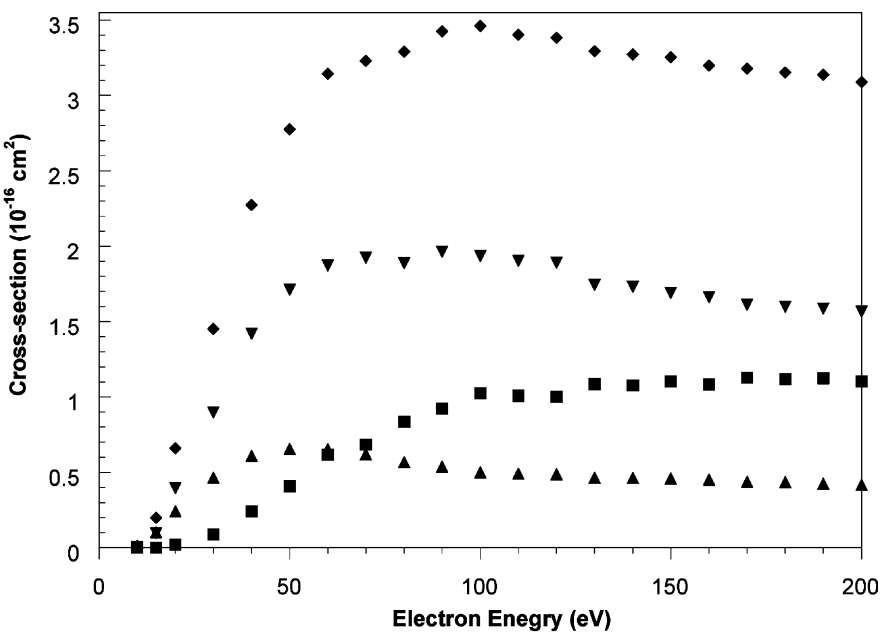

Fig. 5. Present $NO_2{}^+$ (▲), NO^+ (▼), and combined ($N^+ + O^+$) (■) partial ionization cross-sections of NO_2 as a function of electron energy from threshold to 200 eV. Also shown is the sum of the partial cross-sections, which represents the total single NO_2 ionization cross-section (◆).

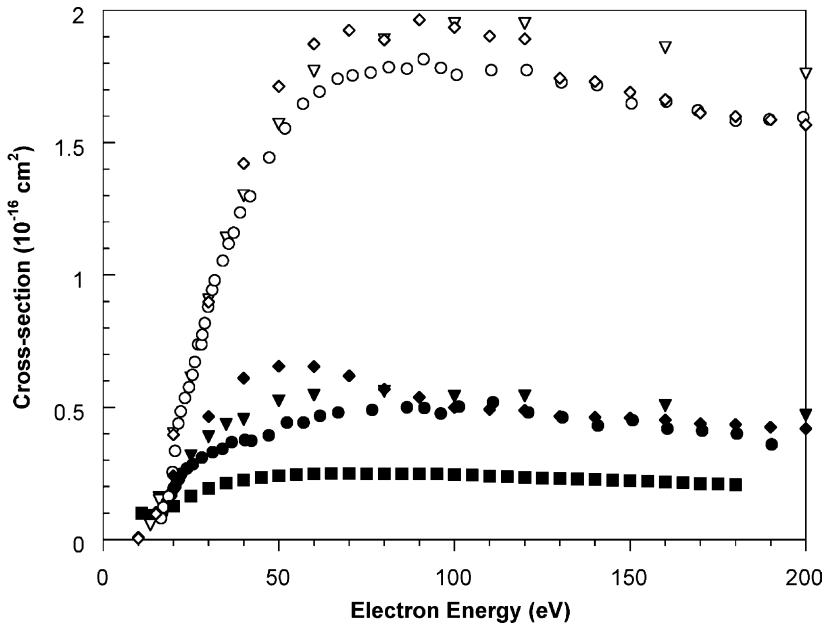

Fig. 6. Present NO_2^+ (◆) and NO^+ (◇) partial ionization cross-section of NO_2 from threshold to 200 eV in comparison with the same cross-section of NO_2^+ from [7] (■), [10] (▼), and [12] (●) and the same corresponding open symbols for NO^+.

the NO_2^+ parent ions and the NO^+ fragment ions in comparison with the measured data of Lindsay et al. [10] and Jiao et al. [12]. For NO_2^+ we also show the data of Stephan et al. [7]. In the case of NO^+ the three different datasets are in good agreement in terms of the absolute cross-section value, but there are slight differences in the energy dependences of the three cross-section functions. As for the formation of the parent NO_2^+ ions, the data of Stephan and co-workers [8] are substantially lower than the other datasets, which, in turn, are in very good agreement with each other at higher impact energies above 100 eV. However, the three cross-section functions show significant differences in their respective low energy behavior. Our data exhibits the largest maximum cross-section value and peak at a lower energy compared to the other two datasets, which also differ in their respective energy dependence. This discrepancy in the cross-section shape is difficult to understand. Fig. 7 shows the present data for the partial cross-section for the formation of $(N^+ + O^+)$ fragment ions in comparison with the data of [10,12]. We note that the authors of [10,12] reported separate cross-sections for the formation of the two atomic fragment ions, which we added up in order to facilitate a comparison with our cross-section for the combined $(N^+ + O^+)$ ion signal. Our $(N^+ + O^+)$ partial cross-section is lower than the other two cross-sections, which have similar maximum values. All three cross-section functions show distinctly different energy dependences, but unlike the case of the NO_2^+ parent ionization cross-section shown in Fig. 6, our $(N^+ + O^+)$ partial cross-section now lies consistently below the other two curves and peaks at a much higher impact energy. Lastly, Fig. 8 summarizes the total NO_2 ionization cross-sections obtained by different investigators in comparison with calculated cross-sections using the DM formalism [15] and the BEB formalism [14]. All cross-section curves have peak cross-section values that are close to each other and range from 3.3×10^{-16} to 3.8×10^{-16} cm^2 which is well within the combined error margins of the experimental datasets. The total cross-sections measured by Lukic et al. [11] and Lindsay et al. [10] and the BEB calculation [14],

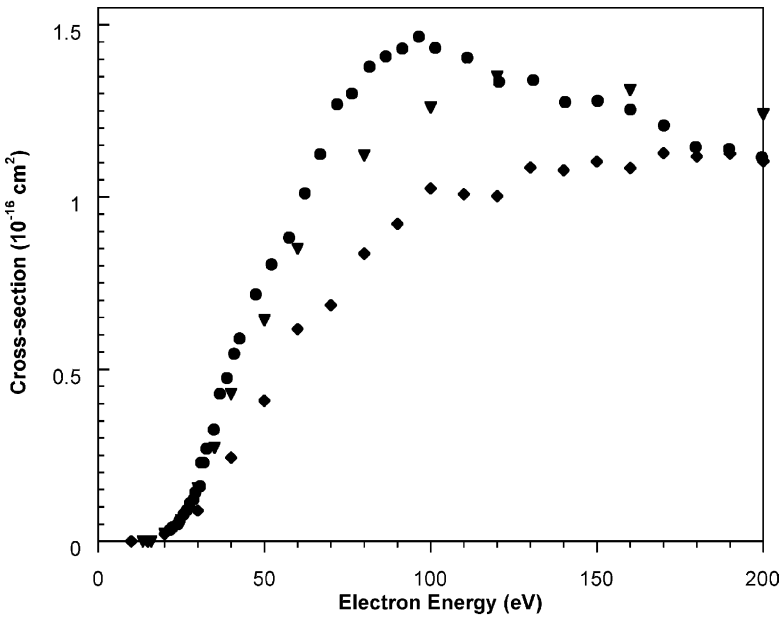

Fig. 7. Present ($N^+ + O^+$) partial ionization cross-section of NO_2 from threshold to 200 eV (◆) in comparison with the same cross-section from [10] (▼) and [12] (●).

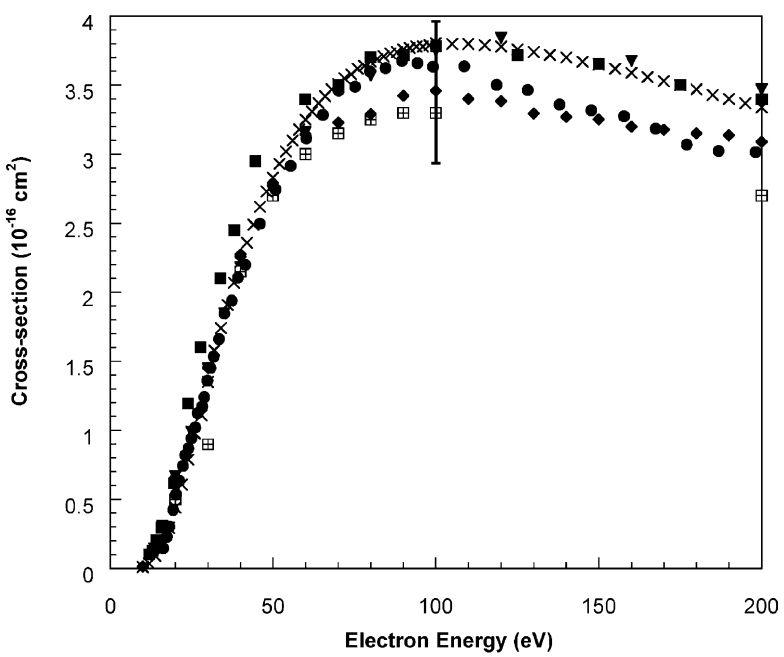

Fig. 8. Present total (single) NO_2 ionization cross-section from threshold to 200 eV (◆) in comparison with the same measured cross-section from [10] (▼), [11] (×), [12] (●), and the calculated NO_2 ionization cross-sections of [14] (■) and [15] (□ with cross). The single error bar refers to a typical margin of uncertainty in the present cross-section.

which have the largest peak cross-section value of 3.8×10^{-16} cm^2 lie essentially on top of each other. Our cross-section curve lies about 10% below those cross-section curves, but exhibits a similar energy dependence (which indicates that the differences in the individual partial cross-sections shapes between our data and those of Lindsay et al. [10] somehow average out!). The cross-section curve of Jiao et al. [12] reaches a maximum value similar to the maximum reported by Lukic et al. [11], Lindsay et al. [10], and the BEB calculation [14], but show a distinctly different energy dependence peaking at lower impact energy and declining much more rapidly with increasing impact energy than the other cross-section curves. The DM calculation [15] follows more closely the present cross-section curve, but declines somewhat more rapidly towards higher impact energies.

3.3. Ionization cross-sections for N_2O

N_2O ("laughing gas") is a linear, triatomic molecule with an even number of electrons. Unlike NO and NO_2, N_2O is not considered an oxide of nitrogen. It has a molecular structure with the oxygen atom at one end and it resonates among three valence-bond structures with double and triple bonds between N and N. This molecular structure of N_2O is such that it cannot be satisfactorily represented by a single valence-bond structure. It can only be reasonably represented by a combination of three stable ground configurations [25]. The ionization cross-section database for this important molecule is rather limited, perhaps because of its peculiar molecular structure. In addition to the total N_2O ionization cross-section measurement of Rapp and Englander-Golden [5], there are the data of Märk et al. [8] for the formation of N_2O^+ parent ions and a set of partial ionization cross-sections reported by Iga et al. [9]. In addition, Kim et al. [14] calculated the N_2O total single ionization cross-section using the BEB method.

Fig. 9 shows the partial N_2O electron-impact ionization cross-sections measured as part of the present work. As in the case of NO, the electron-impact ionization of N_2O is dominated by the formation of the

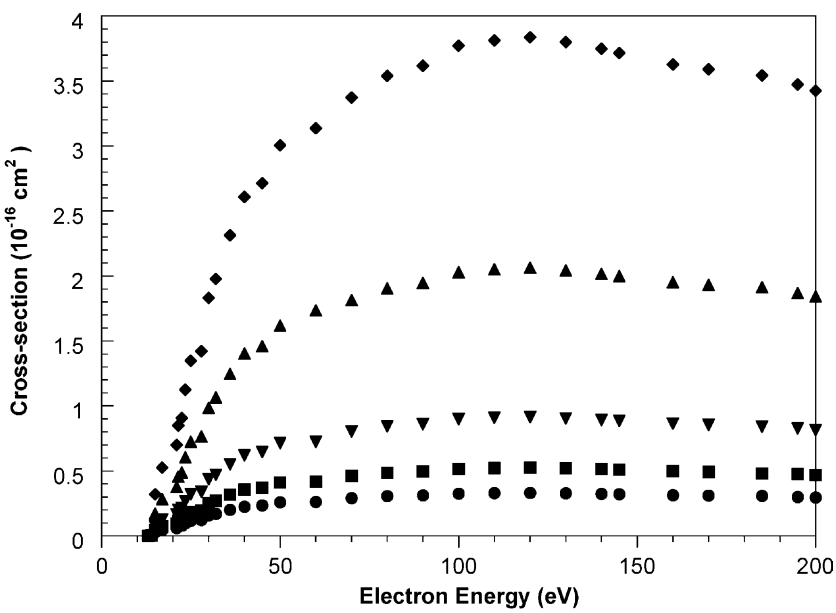

Fig. 9. Present N_2O^+ (▲), NO^+ (▼), N_2^+ (●), and combined ($N^+ + O^+$) (■) partial ionization cross-sections of N_2O as a function of electron energy from threshold to 200 eV. Also shown is the sum of the partial cross-sections (◆), which represents the total single N_2O ionization cross-section, which is essentially identical to the total N_2O ionization cross-section (see text, for details).

parent ion, N_2O^+. However, as one might expect for a triatomic molecule, dissociative ionization channels are more important for N_2O than they were for NO, with appreciable cross-sections for the formation of NO^+, N_2^+, and $(N^+ + O^+)$. As before, we only report a partial cross-section for the formation of the sum of the atomic fragment ions N^+ and O^+ from N_2O as we were also not able to separate the N^+ and O^+ ion signals because of the excess kinetic energy distributions with which these fragment ions are formed. Also shown in Fig. 9 is the sum of the measured partial cross-sections which represents the total single N_2O ionization cross-section (which again is essentially identical to the total N_2O ionization cross-section as the cross-sections for the formation of multiply charged parent or fragment ions are much smaller than those for the formation of singly charged ions). Fig. 10 shows our measured partial N_2O^+ parent cross-section in comparison with data reported by Märk et al. [8] and by Iga et al. [9]. As can be seen, there is excellent agreement between the present data and those of Iga et al. [9] in terms of the absolute cross-section value with a maximum value around 2×10^{-16} cm^2. There is a slight difference in the measured cross-section shapes with our cross-section curve peaking at somewhat higher impact energy. The cross-section curve reported by Märk et al. [8] lays roughly 25% below the other two cross-section curves and has a shape that is similar to the other two cross-section shapes.

Fig. 11 summarizes all dissociative ionization cross-sections of N_2O measured as part of the present study, i.e., NO^+, N_2^+, and $(N^+ + O^+)$ which are shown in comparison with the same partial cross-sections reported by Iga et al. [9]. There is overall very good agreement between the two datasets for all three partial ionization cross-sections in terms of the maximum cross-section values and the cross-section shapes at higher impact energies. However, in all three cases there are significant discrepancies between our cross-section shapes and

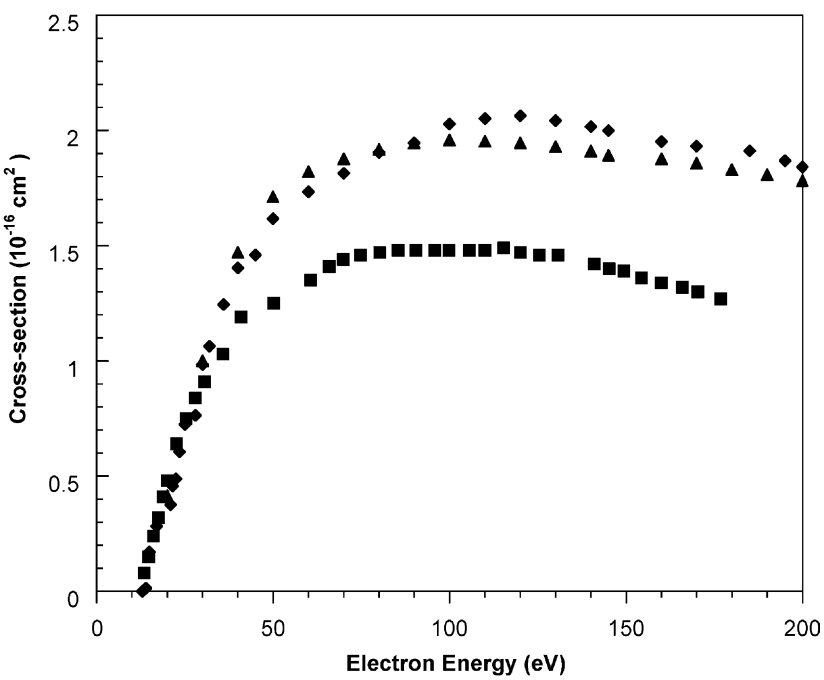

Fig. 10. Present N_2O^+ parent ionization cross-section of N_2O from threshold to 200 eV (◆) in comparison with the same cross-section from [8] (■) and [9] (▲).

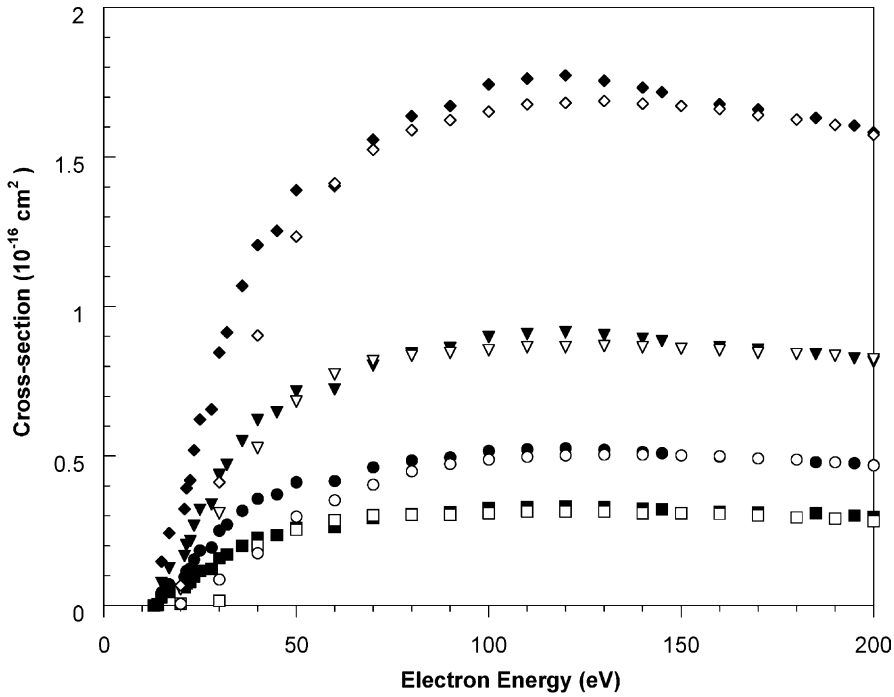

Fig. 11. Present NO^+ (▼), N_2^+ (■), and ($N^+ + O^+$) (●) partial ionization cross-sections from threshold to 200 eV in comparison with the same cross-sections from [9] corresponding open symbols. Also shown are two curves representing the sum of all measured dissociative ionization cross-sections as a function of impact energy; the filled diamonds (◆) represent the present data and the open diamonds (◇) refer to the data of [9].

those of [9] in the low energy regime from threshold to about 50 eV for NO^+ and N_2^+ and up to 80 eV for ($N^+ + O^+$). In general, our measured appearance energies are lower (and closer to the required minimum energies required for the formation of the various fragment ions [21,22,27,28]) than those reported by Iga et al. [9] and our cross-sections rise more rapidly in the near-threshold region. This discrepancy in the cross-section shapes in the low-energy regime is significant as this energy region is particularly important in the modeling and simulation of the electron-driven dissociative ionization processes in, e.g., discharges and plasmas containing N_2O. Also shown in Fig. 11 are two curves representing the sum of all measured dissociative ionization cross-sections. The two curves reflect the behavior of the individual partial dissociative ionization cross-sections. There is excellent agreement between our data and those of [9] in terms of the absolute cross-section values and acceptable agreement in terms of the cross-section shapes except for the low energy region from threshold to about 50 eV where our cross-section lies systematically above the cross-section based on the data reported by Iga et al. [9].

Fig. 12 shows our total single N_2O ionization cross-section in comparison with the measured data from [9] and with the total N_2O ionization cross-section reported by Rapp and Englander-Golden [5]. Also shown is a calculated N_2O ionization cross-section [14] using the BEB formalism. The overall agreement between the various cross-section curves is somewhat better than in the case of NO. The total ionization cross-section reported by Rapp and Englander-Golden [5] has a maximum value of 4.2×10^{-16} cm^2, which is higher than all other data. The present data show a slightly smaller maximum

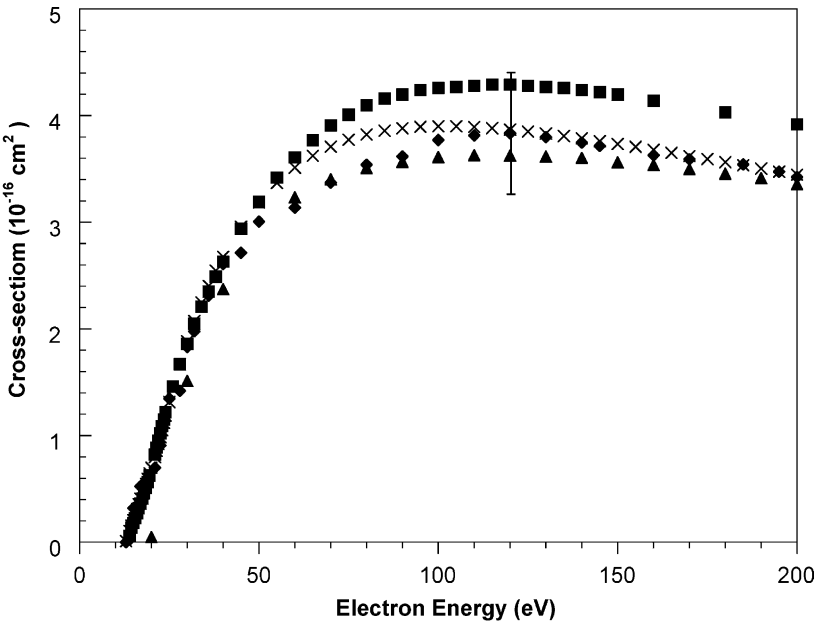

Fig. 12. Present total (single) N_2O ionization cross-section from threshold to 200 eV (◆) in comparison with the same measured cross-section from [9] (▲), the total measured N_2O ionization cross-section of Rapp and Englander-Golden [5] (■), and the calculated N_2O ionization cross-section using the BEB method [14] (×). The single error bar refers to a typical margin of uncertainty in the present cross-section.

cross-section of 3.9×10^{-16} cm^2 and a cross-section shape that is similar to the one reported in [5]. The cross-section curve of Iga et al. [9] shows the lowest peak cross-section with a value of 3.6×10^{-16} cm^2 and a cross-section shape that is somewhat different from the shapes of the other two experimental datasets, in particular at lower impact energies below 50 eV (see discussion above). The calculated N_2O ionization cross-section [14] has a maximum value similar to our value (3.9×10^{-16} cm^2), but the cross-section curves reaches its peak at a somewhat lower impact energy, 80 eV vs. 120 eV in our case and in [5].

4. Conclusions

We measured absolute partial cross-sections for the electron-impact ionization and dissociative ionization of the three nitrogen–oxygen compounds NO, NO_2, and N_2O from threshold to 200 eV using the fast-neutral-beam technique. To the best of our knowledge, this is the first time that ionization cross-sections for all three targets have been measured with the same apparatus using the same experimental technique. Detailed comparisons with other available experimental data and with published calculated total single ionization cross-sections, where available was presented here. In general, the level of agreement between the various reported cross-section sets is not as good as one might expect for simple diatomic and triatomic molecules (see, e.g. [26]). This is particularly true for some of the partial cross-sections for dissociative ionization, in particular in the case of NO_2. There are also differences in the cross-section shapes reported by different authors using different experimental techniques, which tend to be more pronounced for the dissociative ionization cross-sections, but are generally less obvious in the total ionization cross-sections.

Acknowledgements

The work presented in this publication was supported by the Division of Chemical Sciences, Office

of Basic Energy Sciences, Office of Energy Research, U.S. Department of Energy. We also gratefully acknowledge partial support for one of us (V.T.) by the National Aeronautics and Space Administration (NASA) through award NAG5-8971.

References

[1] J.H. Seinfeld, S.N. Pandis, Atmospheric Chemistry and Physics, Wiley, New York, NY, 1998.
[2] E. Boeker, R. van Grondelle, Environmental Physics, Wiley, West Sussex, England, 1995.
[3] T.L. Brown, H.E. Lemay, B.E. Bursten, Chemistry, The Central Science, 7th ed., Prentice Hall, Upper Saddle River, NJ, 1997.
[4] D.D. Reible, Fundamentals of Environmental Engineering, CRC Press, Boca Raton, FL, 1999.
[5] D. Rapp, P. Englander-Golden, J. Chem. Phys. 43 (1965) 1464.
[6] Y.D. Kim, K. Stephan, E. Märk, T.D. Märk, J. Chem. Phys. 74 (1981) 6771.
[7] K. Stephan, H. Helm, Y.B. Kim, G. Seykora, J. Ramler, M. Grössl, E. Märk, T.D. Märk, J. Chem. Phys. 73 (1980) 303.
[8] E. Märk, T.D. Märk, Y.D. Kim, K. Stephan, J. Chem. Phys. 75 (1981) 4446.
[9] I. Iga, M.V.V.S. Rao, S.K. Srivastava, J. Geophys. Res. 101 (1996) 9261.
[10] B.G. Lindsay, M.A. Mangan, H.C. Straub, R.F. Stebbings, J. Chem. Phys. 112 (2000) 9404.
[11] D. Lukic, G. Josifov, M.V. Kurepa, Int. J. Mass Spectrom. 205 (2001) 1.
[12] C.Q. Jiao, C.A. DeJoseph Jr., A. Garscadden, J. Chem. Phys. 117 (2002) 161.
[13] W. Hwang, Y.-K. Kim, M.E. Rudd, J. Chem. Phys. 104 (1996) 2956.
[14] Y.-K. Kim, W. Hwang, N.M. Weinberger, M.A. Ali, M.E. Rudd, J. Chem. Phys. 106 (1997) 1026.
[15] M. Probst, H. Deutsch, K. Becker, T.D. Märk, Int. J. Mass Spectrom. 206 (2001) 13.
[16] V. Tarnovsky, P. Kurunczi, D. Rogozhnikov, K. Becker, Int. J. Mass Spectrom. Ion Process. 128 (1993) 181.
[17] V. Tarnovsky, K. Becker, J. Chem. Phys. 98 (1993) 7868.
[18] R.C. Wetzel, F.A. Biaocchi, T.R. Hayes, R.S. Freund, Phys. Rev. A 35 (1987) 559.
[19] R.S. Freund, R.C. Wetzel, R.J. Shul, T.R. Hayes, Phys. Rev. A 41 (1990) 3575.
[20] V. Tarnovsky, K. Becker, Z. Phys. D 22 (1992) 603.
[21] S.G. Lias, J.E. Bartmess, J.F. Liebman, J.L. Holmes, R.D. Levine, W.G. Mallard, J. Phys. Chem. Ref. Data 17 (1988) 1.
[22] D.D. Wagman, W.H. Evans, V.B. Parker, R.H. Schumm, I. Halow, S.M. Bailey, K.L. Chuney, R.L. Nutall, J. Phys. Chem. Ref. Data 11 (1982) 1.
[23] SIMION, Version 5.0, Idaho National Engineering Laboratory, EG&E Idaho Inc., Idaho Falls, ID, 1992;
SIMION-3D, Version 6.0, Science and Technology Software Center, 1996.
[24] J.C. Speakman, Molecules, McGraw-Hill, New York, NY, 1966.
[25] L. Pauling, The Nature of the Chemical Bond, 3rd ed., Cornell University Press, Ithaca, NY, 1960.
[26] H. Deutsch, K. Becker, S. Matt, T.D. Märk, Int. J. Mass Spectrom. 197 (2000) 37.
[27] M.W. Chase Jr., K.A. Davis, J.R. Downey, D.J. Frurip, R.A. McDonald, A.N. Syverud, J. Phys. Chem. Ref. Data 14 (1985) 1.
[28] R.C. Weast, M.J. Astle, W.H. Beyer (Eds.), The Handbook of Chemistry and Physics, 65th ed., CRC Press, Boca Raton, FL, 1985.